



# Effect of Low-Level Laser Irradiation (810 nm) on the Proliferation and Differentiation of Osteoblast-Like Cells Cultured on SLA Titanium Discs Exposed to a Peri-implantitis Environment

Evangelia P. Zampa<sup>1\*</sup>, Kyriaki Kyriakidou<sup>1</sup>, Joseph Papaparaskevas<sup>2</sup>, Eudoxie Pepelassi<sup>1</sup>, Ioannis K. Karoussis<sup>1</sup>

<sup>1</sup>Department of Periodontology, School of Dentistry, National and Kapodistrian University of Athens, Thivon 2 Str, Goudi, 115 27, Athens, Greece

<sup>2</sup>Department of Microbiology, School of Medicine, National and Kapodistrian University of Athens, M.Asias 75, 115 27, Athens, Greece

\*Correspondence to  
Evangelia P. Zampa,  
Email: [elina\\_zampa@windowslive.com](mailto:elina_zampa@windowslive.com)

Received: July 19, 2023  
Accepted: October 7, 2023  
ePublished: November 26, 2023

## Abstract

**Introduction:** Elimination of inflammation and re-osseointegration are the major objectives of peri-implantitis therapy. Existing data, however, do not support any decontamination approach. Thus, the present *in vitro* study aims to assess whether the air-debriding decontamination method with erythritol powder restores the biocompatibility of infected titanium discs and to investigate the potent biomodulatory ability of diode laser (810 nm) irradiation to promote cell proliferation and differentiation of premature osteoblast-like cells (MG63) towards osteocytes.

**Methods:** The experimental groups consisted of cells seeded on titanium discs exposed or not in a peri-implantitis environment with or without biomodulation. Infected discs were cleaned with airflow with erythritol powder. Cell cultures seeded on tricalcium phosphate (TCP) surfaces with or without biomodulation with a laser (810 nm) were used as controls. The study evaluated cell viability, proliferation, adhesion (SEM) at 24, 48 and 72 hours, and surface roughness changes (profilometry), as well as the effects of low-level laser therapy (LLLT) on ALP, OSC, TGF- $\beta$ 1, Runx-2, and BMP-7 expression in MG63 cells' genetic profile on days 7, 14, and 21.

**Results:** The MTT assay as well as the FDA/PI method revealed that cell proliferation did not show significant differences between sterile and decontaminated discs at any timepoint. SEM photographs on day 7 showed that osteoblast-like cells adhered to both sterile and disinfected surfaces, while surface roughness did not change based on amplitude parameters. The combination of airflow and LLLT revealed a biomodulated effect on the differentiation of osteoblast-like cells with regard to the impact of laser irradiation on the genetic profile of the MG63 cells.

**Conclusion:** In all groups tested, osteoblast-like cells were able to colonize, proliferate, and differentiate, suggesting a restoration of biocompatibility of infected discs using airflow. Furthermore, photomodulation may promote the differentiation of osteoblast-like cells cultured on both sterile and disinfected titanium surfaces.

**Keywords:** Peri-implantitis; Airflow; LLLT; Biomodulation; Photomodulation.



## Introduction

An inflammation of the peri-implant mucosa and a progressive loss of the supporting bone are two characteristics of the pathological condition known as peri-implantitis, being irreversible or reversible up to a specific grade depending on the damage of peri-implant tissues.<sup>1</sup> According to a recent systematic review and meta-analysis, the mean prevalence of peri-implantitis is 12.53% for implant-level and 19.53% for patient-level.<sup>2</sup>

The attainment of re-osseointegration is the ultimate objective in the treatment of peri-implantitis, in addition to the eradication of inflammation and the removal of

biofilm from the implant surface. In light of this, the optimal surface decontamination technique should not only eliminate contaminants but also maintain surface micromorphology in terms of roughness, free energy, and composition.<sup>3</sup> However, limited existing data do not endorse any particular implant surface decontamination method over the others for either non-surgical<sup>4</sup> or surgical peri-implantitis therapy.<sup>5,6</sup>

Airflow/Perioflow has been introduced as an alternative and promising physicommechanical approach for the supra- and submucosal cleansing of titanium implants with the least structural changes on the implant

surface and the lowest titanium abrasion.<sup>7,8</sup> An *in vitro* study by Matsubara et al aimed to compare small (glycine and erythritol) and larger-sized (sodium bicarbonate) powders in terms of cleaning capacity.<sup>9</sup> Both the implant collar and the roughness of implant threads were significantly increased by sodium bicarbonate.

Low-level laser therapy (LLLT) enhances cell proliferation and differentiation in sterile rough or smooth discs using either the GaAlAs diode (830 nm or 780 nm) or the Nd: YAG (1064 nm) laser, as it was revealed by the increased gene expression of ALP, OSC, TGF- $\beta$ 1, OSC, BSP, and BMP-7.<sup>10-12</sup> Up to now, there has been no published research on the effect of LLLT on decontaminated implant surfaces, previously exposed to a peri-implantitis environment.

The objective of the current *in vitro* study was to assess if employing airflow for disinfection may potentially restore the biocompatibility of infected titanium discs. Additionally, the purpose of this study was to evaluate the potential biomodulatory impact of diode laser (810 nm) radiation on the differentiation and proliferation of premature osteoblast-like cells (MG63).

## Materials and Methods

### Titanium Discs

200 titanium discs with a Straumann® surface that had been acid-etched and sandblasted (large grid) (SLA) were used. All samples were manufactured from commercially pure Titanium grade II. Discs were prepared from 1mm thick sheets and were fabricated to fit into the well of a 24-well cell culture plate (approx. 15 mm in diameter). Discs were sterilized under  $\gamma$ -radiation.

### Contamination of Titanium Discs

The contamination of titanium discs was performed by the co-culture of anaerobic bacterial strains detected in the dental plaque. The German Collection of Microorganisms and Cell Cultures (DSMZ) was utilized to obtain the microbiological strains *Streptococcus oralis*-DSM 20627, *Actinomyces naeslundii*-DSM 43013, *Veillonella dispar*-DSM 20735, and *Porphyromonas gingivalis*-DSM 20709. The bacteria were grown in anaerobic conditions (80% N<sub>2</sub>, 10% H<sub>2</sub>, 10% CO<sub>2</sub>) at 37 °C in a nutritional medium (Brain Heart Infusion medium - BHI), enhanced with 10 g/mL vitamin K.<sup>13</sup>

The optical densities of bacterial cultures were measured using a McFarland Nephelometer and were adjusted to 0.1. For the bacterial co-culture, the suspension with optical density (OD<sub>600</sub>=0.1) of each bacterium was mixed with BHI and vitamin K so that the optical density of the suspension was 0.01 (OD<sub>600</sub>=0.01). 500  $\mu$ L of suspension mixture with 50 mL of BHI and vitamin K were placed in each plate containing one disc. Then, the multi-well plate was placed into a plastic incubation chamber under anaerobic conditions which were

achieved using hypoxic envelopes, and it remained for 48 hours at 37 °C.<sup>13</sup>

### Experimental and Control Groups

The experimental groups were the following:

- Group I: Sterile SLA titanium discs without any intervention, where osteoblast-like cells were seeded on their surface.
- Group II: SLA titanium discs coated with biofilm were decontaminated with airflow seeded with osteoblast-like cells.
- Group III: Sterile SLA titanium discs without any intervention, where osteoblast-like cells were seeded on the surface and irradiated with LLLT.
- Group IV: SLA titanium discs coated with biofilm were decontaminated with airflow seeded with osteoblast-like cells irradiated with LLLT.

The control groups were the following:

- Group V: Osteoblast-like cells seeded on TCP irradiated with LLLT.
- CTRL: Osteoblast-like cells seeded on TCP.

### Application of Airflow

The AirFlow Master Piezon device from EMS, Nyon, Switzerland, and the powder AirFlow Pulver Plus (erythritol 14 $\mu$ m, amorphous silicon and chlorhexidine 0.3%) were used. The distance between the edge of the handpiece and the titanium discs was 5  $\pm$  1 mm; the angle was approximately 45° in relation to the disc surface, and the application lasted 90". The water and air supply were set to maximum intensity. Then, saline was used to wash up the discs for 30" each.

Discs were placed, according to the experimental groups, in separated sterilization sachets and were autoclaved before cell cultures.

### Cell Line

MG63 human osteoblast-like cells (LGC standards, Germany) were grown and maintained in Dulbecco's Modified Eagle Medium (DMEM - Gibco Grand Island, NY) low glucose, 10% fetal bovine serum (FBS), and enriched with 1% antibiotics solution (penicillin-streptomycin Sigma-Aldrich, Ge) in a controlled environment (5% CO<sub>2</sub>, 37 °C). Between the third and fourth passages, MG63 cells were planted in 24-multiwell plates at a density of 1  $\times$  10<sup>4</sup> cells/cm<sup>2</sup>. Osteoblast-like cells were cultured in all the experimental groups and controls for 24, 48 and 72 hours for the MTT assay and FDA/PI staining, and for 7, 14 and 21 days in order to assess gene expression.

### LLLT Application

24 hours after culture, MG63 cells were irradiated with an 810 nm diode laser (Fotona, Ljubljana, Slovenia) via the optical fiber of 300  $\mu$ m (Table 1). To irradiate

**Table 1.** Specific Diode Laser Settings Applied in the Study

Parameter	Value
Type of laser	Diode
Emission mode	Continuous wave
Wavelength	810 nm
Delivery system	Optical fiber 300 µm
Power	500 mW
Distance from the surface	10 mm
Spot diameter at the well	4.6 mm
Spot area at the well	0.16 cm <sup>2</sup>
Irradiation time	96 seconds
Energy density at the spot area	300 J/cm
Energy density at the well	15 J/cm

the multi-well plate, we moved the laser in circular, concentric motions at a distance of 10 mm of the optical fiber from the surface of the culture. Our research team investigated the irradiation parameters in earlier experiments: 500 mW for 96 seconds and 300 J/cm<sup>2</sup> of energy density.<sup>14</sup>

#### MTT Assay

The cell viability of the experimental groups was assessed by using the MTT assay which measures metabolic activity dependent on cell numbers; thus, it is considered indicative of cell proliferation. At each endpoint, 200 µL of phenol-free media were added to the cells, containing 5 µg/mL solution of the MTT reagent, and incubated for 4 hours. The developed formazan crystals were solubilized in isopropanol acidified with 1% HCl.

The absorbance was then measured using a SpectraMax microplate reader (Molecular Devices, Silicon Valley, California, USA) at 570 and 690 nm.

#### FDA/PI Staining

The double staining FDA/PI (Sigma-Aldrich, Ge) approach was used to assess cell apoptosis. 10 ml of PBS was combined with 5 µL of a dysoxic fluorescein solution and 2 µL of iodine propidium. Each well received 1 mL of the solution, which was then incubated for 3 minutes at room temperature in a dim, humid environment. Living cells showed up as green (FDA stain) on the fluorescent microscope (Olympus BX60), while dead cells showed up as red (PI stain).

#### Scanning Electron Microscope

In order to evaluate osteoblasts' adhesion to the samples' surface and exhibiting morphology, scanning electron microscope (SEM) was used (FEI, QUANTA INSPECT, USA). SEM microphotographs were obtained from the central area of the discs at 500x, 1000x and 1500x magnifications with low beam intensity of electrons, voltage 25 kV on days 7, 14 and 21.

#### Profilometric Analysis

The surface morphology of airflow-decontaminated, autoclaved, and sterile discs was evaluated. An optical profiler (Wyko NT 1100, Veeco, Tuscon, AZ, USA) operating in vertical scanning mode with a Mirau lens at a 20 magnification (sample area: 231.1 µm 303.8 µm) evaluated the three-dimensional surface roughness of the specimens (n=5/group). Each specimen underwent five measurements, which were averaged. The surface parameters assessed included both amplitude (Sa, average roughness; Sq, maximum height of the surface; Sz, average of maximum height of the hills to valleys; Sku, sharpness of the height distribution; Ssk, degree of the bias of the roughness shape) and hybrid (Sdq, root mean square of slopes at all points in the definition area; Sdr, percentage of the additional surface area in the definition area contributed by the texture as a whole; Sds, number of summits per unit area making up the surface; Ssc, mean summit curvature for the various peak structures and Str).

#### Evaluation of the Gene Expression of Osteoblast-Like Cells

##### RNA Extraction and cDNA Synthesis

RNA extraction was performed using the TRitidy G RNazol solution (Applichem, Cinisello Balsamo, Milano). Following the extraction, the RNA was quantified using nanodrop photometer NanoDrop™ One (Thermo Fisher Scientific, USA).

Following the manufacturer's instructions, reverse transcription was carried out using 1µg of total RNA and the protoscript II first strand cDNA synthesis kit (NEB, US). The cDNA was kept at -20 °C.

##### Quantitative Polymerase Chain Reaction Analysis

SYBR green chemistry and specific primers for the genes ALP, OSC, TGF-1, BMP-7, and Runx-2 were used in quantitative polymerase chain reaction (qPCR) to measure gene expression (data not shown). A Stratagene real-time cyclor (Agilent Technologies, IT) was used to conduct the analysis. The study was conducted using the DDcT technique for relative quantification after the expression was standardized to GAPDH. The amplification curves of each sample were used to determine the cycle threshold (Ct) and melt curves to confirm the creation of a particular product.

##### Statistical Analysis

All experiments were performed in triplicate in three independent runs. The data were proportional, and they were expressed as mean values ± standard error of the mean which quantifies uncertainty in the estimate of the mean. Differences between the groups were analyzed with the analysis of variance (ANOVA) parametric test. Differences per pair of groups were evaluated with Tukey's test, while the differences between the groups

in the different timepoints were evaluated by ANOVA and then with a post-hoc test with the application of Bonferroni correction. The statistical significance was set at  $P=0.05$ .

Concerning profilometric analysis, descriptive analysis was performed using means and standard deviations. Kolmogorov–Smirnov normality was performed, while intergroup comparisons were performed via one-way ANOVA and Friedman test followed by Dunns post-tests (GraphPad Prism).

**Results**

**Evaluation of Cell Viability and Proliferation**

MTT assay indicated an increase in cell proliferation at all timepoints. More specifically, at 24 hours group I showed a statistically significantly lower MTT value compared to groups I II, IV, V and CTRL (Figure 1). In addition, Group III showed no statistically significant differences compared to experimental groups but only to control ones. Group V showed a statistically significantly higher MTT value compared to all other groups.

At both 48 and 72 hours, groups I, II, III, and IV presented a statistically significantly lower MTT value compared to groups V and CTRL (Figure 1). The FDA/PI staining of MG63 cells confirmed the results of the MTT assay and the increase of cell proliferation in the three timepoints. In Figure 2, fluorescent microscope representative images are presented, reporting FDA/PI dyes on the experimental surfaces at 72 hours. In addition, the histogram reports the evaluation of alive/dead cells, using the Image J program, based on the reported images.

**Evaluation of Cell Adhesion and Morphology**

Scanning electron microphotographs of MG63 cells cultured on titanium surfaces (1000×) on day 7 showed osteoblast-like cells actively adhered to all surfaces with a combination of cells of flat morphology in close contact with the surface with cytoplasmic prolongations and filopodia [Figure 3 (a,d)], more rounded or cuboid, with shorter prolongations [Figure 3 (b,c)].

On day 14, a greater number of cells could be seen in all groups, while irradiated groups (II and IV) had more cells

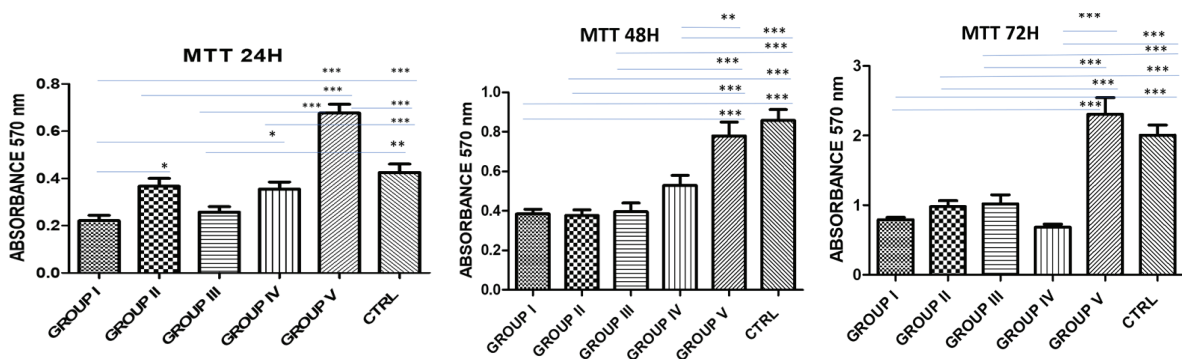


Figure 1. MTT Assay at 24, 48 and 72 Hours. \*  $P<0.05$ , \*\*  $P<0.005$ , \*\*\*  $P<0.0005$

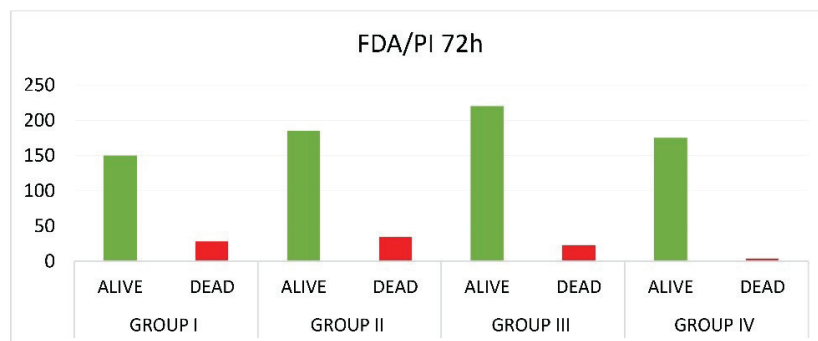
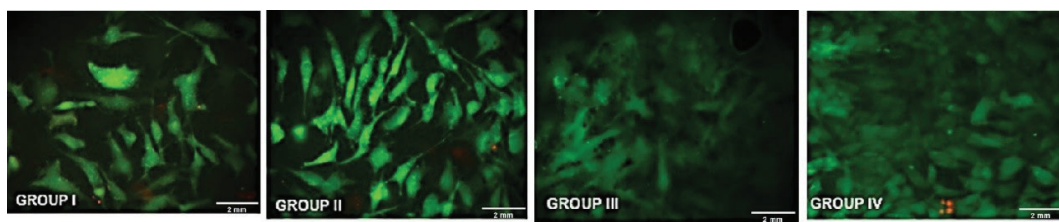


Figure 2. Florescent Microscope Images Reporting FDA/PI Staining of MG63 Cells Seeded on the Experimental Surfaces at 72 Hours. The histogram Reports the Evaluation of Alive/Dead Cells

with regular morphology. On day 21, overpopulation including both osteocytes and osteoblasts was detected (data not shown).

**Evaluation of Surface Roughness**

The results of the profilometric analysis showed no statistically significant differences between the tested specimens in all amplitude parameters. Concerning hybrid parameters, Sdq and Sdr values of sterile discs were statistically significantly higher compared to autoclaved discs, while the Ssc value of both sterile and autoclaved

discs was statistically significantly higher compared to disinfected discs (Figure 4).

**Evaluation of Osteoblast Gene Expression**

For the evaluation of gene expression levels, only cultures on TCP were used as controls, whereas MG63 cells seeded on TCP and irradiated with LLLT (group V) were used as covariant.

**ALP Gene Expression**

Intragroup analysis of qPCR on days 7, 14, and 21 revealed

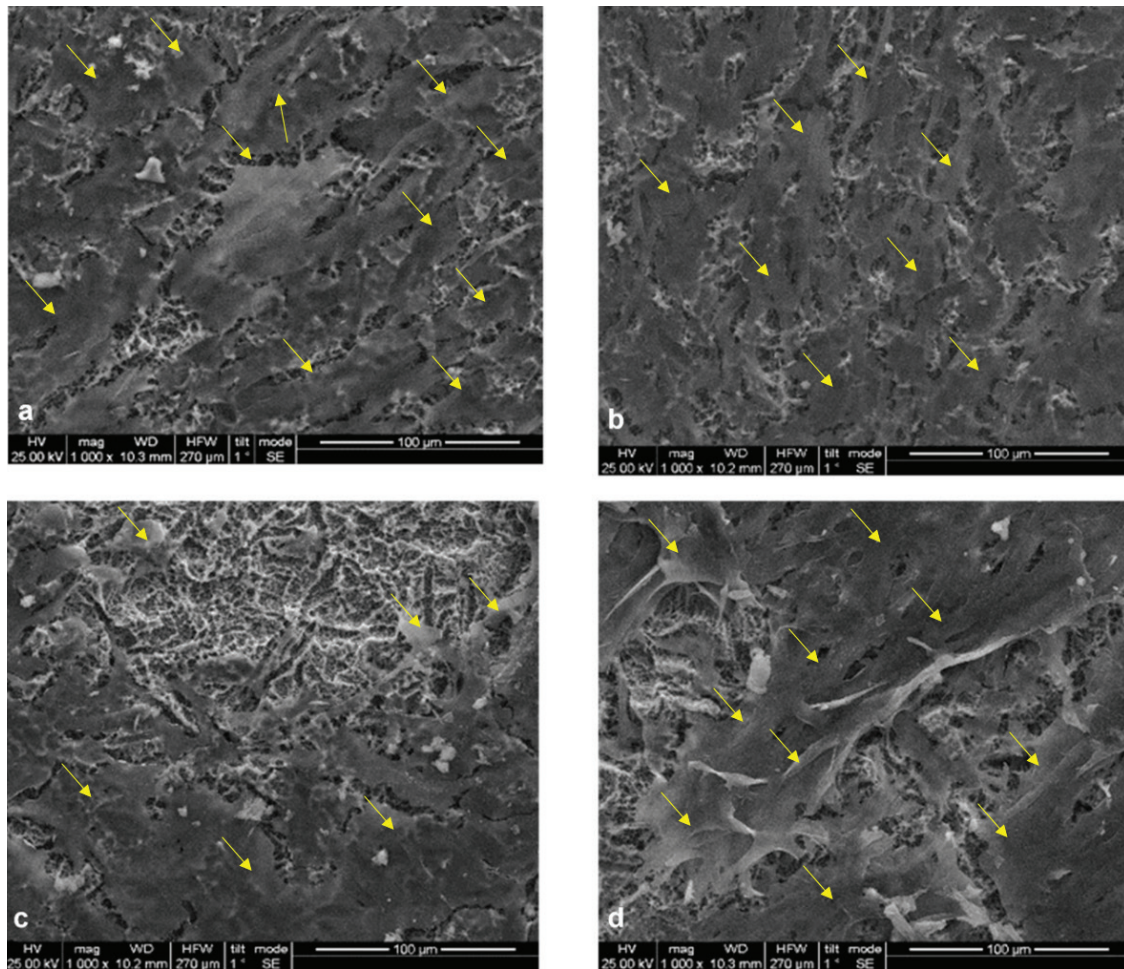


**Figure 3.** Scanning Electron Microphotographs of MG63 Cells (1000 ×) on Day 7. (a) group I, (b) group II, (c) group III and (d) group IV. Arrows determine the location of some of the osteoblast-like cells

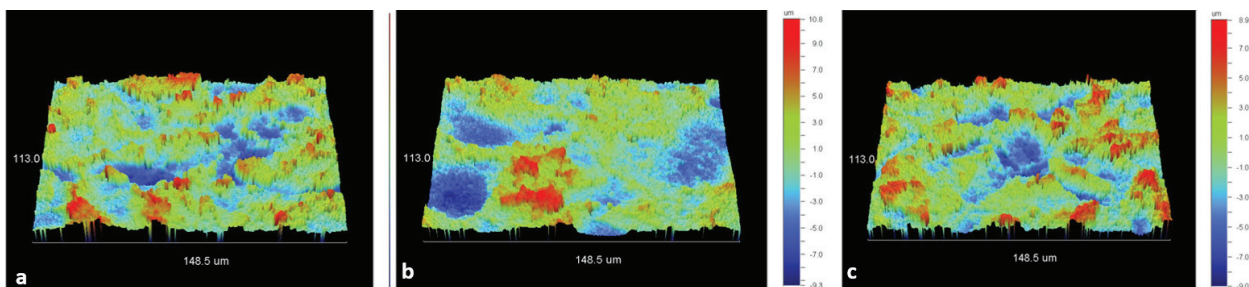


**Figure 4.** Roughness Parameters of Titanium Discs Surface and Dimensional Interactive Display: (a) Sterile, (b) Autoclaved, (c) Decontaminated with airflow

that ALP expression increased in all tested groups on days 7 and 14, while on day 21 a significant reduction was obvious (data not shown).

The intergroup analysis on day 7 (Figure 5) showed that groups II, III and IV presented a statistically significantly higher expression of ALP compared to group I. On day 14, ALP expression for group I remained lower. However, this difference reached statistical significance only for group IV. On day 21, ALP expression was statistically significantly reduced compared to group V.

**OSC Gene Expression**

The results of intragroup analysis of qPCR in the three timepoints showed a gradual increase of OSC expression on days 7, 14 and 21 in all groups (data not shown).

The intergroup analysis on day 7 showed no statistically significant difference between the experimental groups, while on day 14 a statistically significantly lower expression was expressed in group I compared to groups III, IV, and V (Figure 6). Moreover, a statistically

significant difference was observed between group II and groups III, IV, and V with group II showing a statistically significantly lower expression value compared to the other three groups. Finally, group III showed a statistically significantly lower expression value compared to both groups IV and V.

On day 21, group I showed a statistically significantly lower expression value compared to groups III, IV, and V (Figure 6). Additionally, group II showed a statistically significantly lower expression value compared to group IV.

**TGF-β1 Gene Expression**

The results of intragroup analysis of qPCR in the three timepoints showed an increase of TGF-β1 expression in all experimental groups on days 7 and 14, while a decrease on day 21 was observed (data not shown).

The intergroup analysis on day 7 revealed that group I showed a statistically significantly lower expression value compared to group III (Figure 7). In addition, group

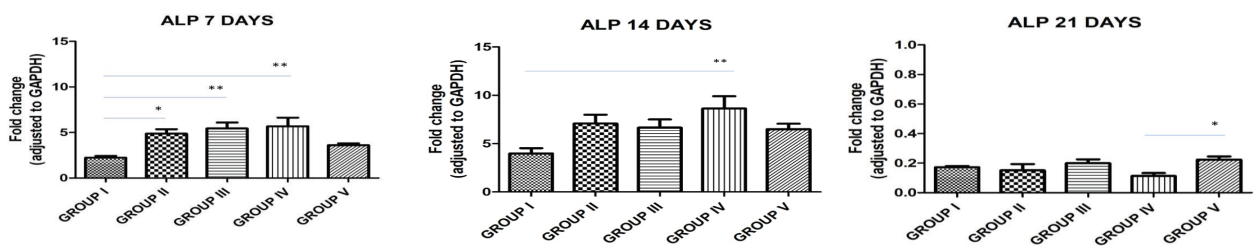


Figure 5. ALP Expression on Days 7, 14 and 21. \*  $P < 0.05$ , \*\*  $P < 0.005$ , \*\*\*  $P < 0.0005$

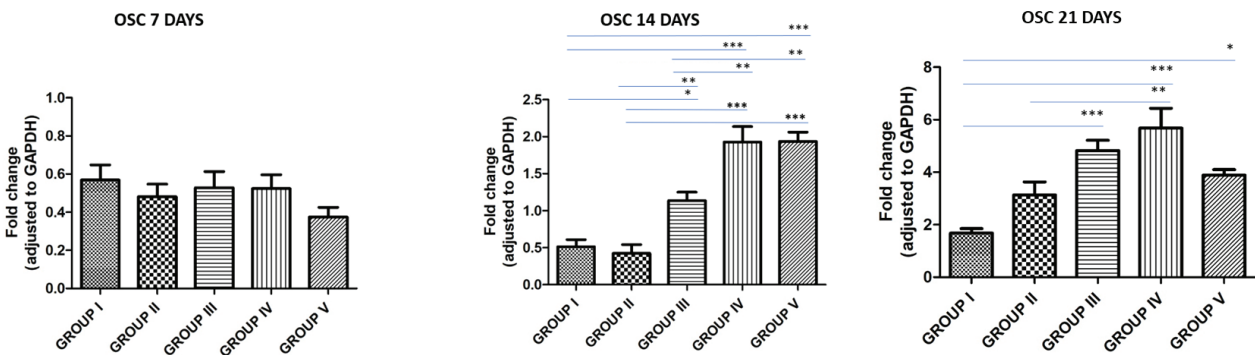


Figure 6. OSC Expression on Days 7, 14 and 21. \*  $P < 0.05$ , \*\*  $P < 0.005$ , \*\*\*  $P < 0.0005$

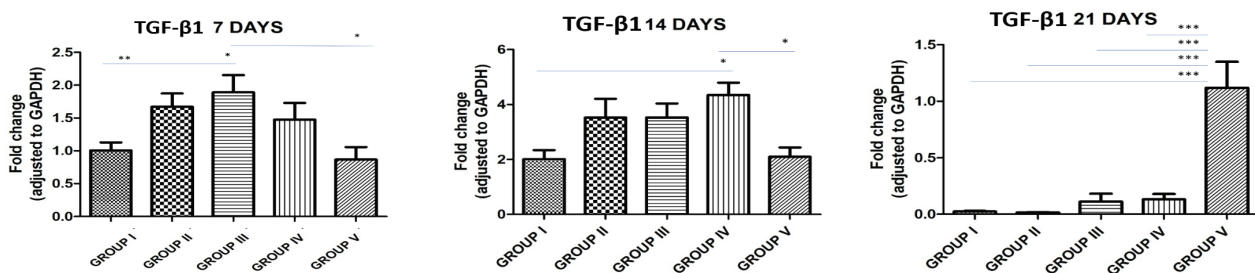


Figure 7. TGF-β1 Expression on Days 7, 14 and 21. \*  $P < 0.05$ , \*\*  $P < 0.005$ , \*\*\*  $P < 0.0005$

III showed a statistically significantly higher expression value compared to group V.

On day 14, group I showed a statistically significantly lower expression value compared to group IV. In addition, group IV showed a statistically significantly higher expression value compared to group V.

On day 21, a substantial reduction of TGF- $\beta$ 1 expression was found for all groups. However, TGF- $\beta$ 1 was significantly higher for group V compared to all other groups.

### Runx-2 Gene Expression

Expression level values of groups I, III, IV and V increased on days 7 and 14, while group II showed a gradual decrease. On day 21, all groups showed a decrease in their expression values except group I which showed an increase (data not shown).

Concerning the intergroup analysis, on day 7 no statistically significant difference was observed between the experimental groups, while on day 14 group IV showed a statistically significantly higher expression value compared to groups I, II, III, and V (Figure 8). In addition, a statistically significant difference was observed between group II and group III, as group III showed a statistically significantly higher expression value.

Finally, on day 21 group I showed a statistically significantly higher expression value compared to all the other groups.

### BMP-7 Gene Expression

Groups I and V showed an increase in BMP-7 expression

on days 7, 14 and 21, while groups II, III and IV showed a gradual decrease on days 14 and 21 (data not shown).

The intergroup analysis on day 7 showed a statistically significant difference between group IV and groups I, II, III, and V, while group IV showed a higher expression value compared to the other four groups (Figure 9).

On day 14, group IV showed a statistically significantly higher expression value compared to groups II and III.

On day 21, group I showed a statistically significantly higher expression value compared to groups II, III, and IV, while group V showed a statistically significantly higher expression value compared to groups II, III, and IV.

### Discussion

As far as we are aware, this is the first study examining the impact of LLLT on decontaminated implant surfaces, previously exposed to a peri-implantitis environment. Moreover, this study investigated the restoration of the biocompatibility of infected implant surfaces, after decontamination using airflow with erythritol powder.

The study evaluated the cell viability and proliferation of osteoblast-like cells by using the MTT assay and FDA/PI staining, adhesion and cell morphology in all experimental groups performing SEM, and surface roughness changes via profilometry. qPCR was used to analyze the genetic profile of the MG63 cells as well as the results of low-level laser irradiation. More particularly, evaluations were made of the expression of ALP, OSC, TGF- $\beta$ 1, Runx-2, and BMP-7.

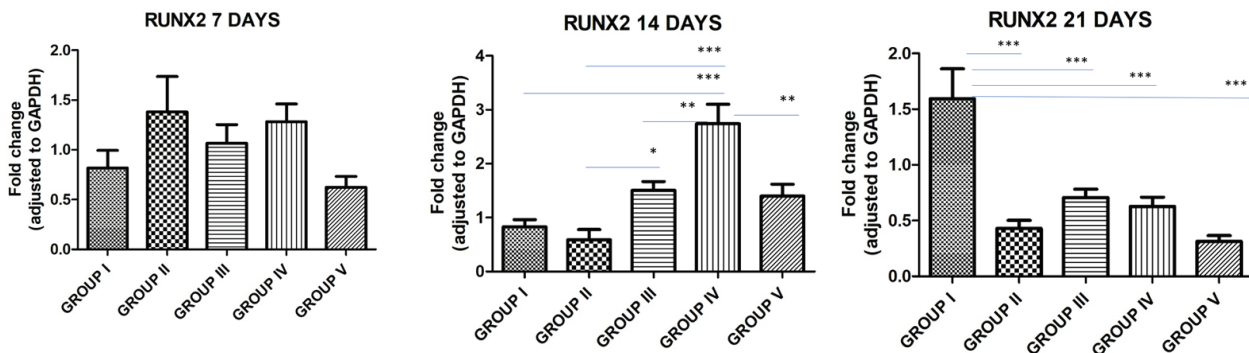


Figure 8. Runx-2 Expression on Days 7, 14 and 21. \*  $P < 0.05$ , \*\*  $P < 0.005$ , \*\*\*  $P < 0.0005$

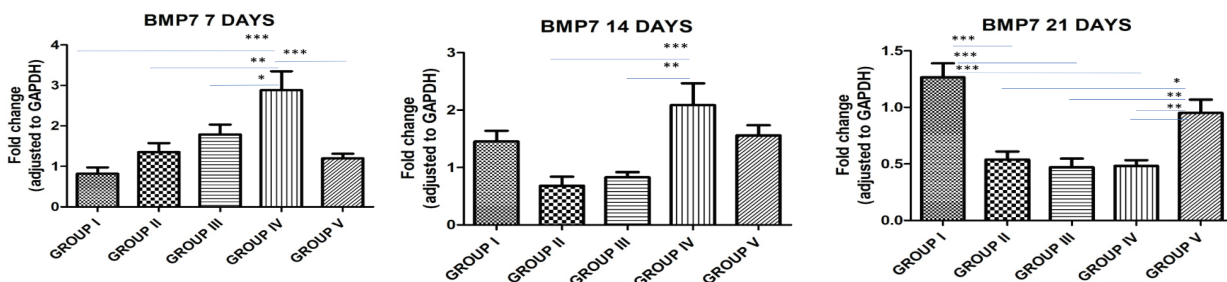


Figure 9. BMP-7 Expression on Days 7, 14 and 21. \*  $P < 0.05$ , \*\*  $P < 0.005$ , \*\*\*  $P < 0.0005$

Based on the results of the MTT assay, the proliferation of osteoblast-like cells increased gradually from 24 to 72 hours in all groups of the study. These findings were verified by FDA/PI staining. At 24 hours, the greatest increase was observed in group V in which TCP acts as the best culture surface in combination with the beneficial effect of LLLT.<sup>15</sup> Interestingly, decontamination by the application of airflow with erythritol powder led to titanium surfaces, previously exposed to a peri-implantitis environment, which allowed cell adhesion similar to what was expected on sterile surfaces as revealed by Scanning Electron Microscopy. The cell adhesion and morphology of osteoblast-like cells cultured on decontaminated surfaces did not differ compared to what was observed on surfaces that had never been exposed to the deleterious effects of microbes. The results showed that on day 7 MG63 cells were actively adhered to all surfaces with a combination of cells of flat morphology in contact with the surface with cytoplasmic prolongations and filopodia and cells rounded or cuboid with shorter prolongations. Irradiated groups (III and IV) had cells with more regular morphology, a finding that was also confirmed on day 14. On day 21, overpopulation, including both osteocytes and osteoblasts, was detected in all groups. These findings are indicative of restored biocompatibility on the implant surface of the previously infected implant surface. The restoration of biocompatibility was supported by the results of MTT assay and FDA/PI staining where no differences in the cell proliferation and living/dead cell ratio were found between sterile and disinfected titanium surfaces.

This finding differs from John and colleagues' study which indicated that although air abrasion is efficient for biofilm removal from titanium surfaces, the reestablishment of biocompatibility after biofilm formation and decontamination cannot be restored on titanium surfaces.<sup>16</sup> However, in this study there were several differences that may explain the inability to restore biocompatibility. These differences include the vertical application of the aerosol derived from the handpiece, the powders evaluated, and the lack of rinsing of saline after decontamination for the removal of powder remnants. The powders tested contained glycine, sodium bicarbonate, and/or tricalcium phosphate (TCP). All these substances are provided in large particles (<40  $\mu\text{m}$ ) while erythritol powder used in the present study consists of small particles of 14 $\mu\text{m}$ . This powder combined with the perpendicular direction of the air mixture may cause changes on the implant surface. After all, surface modifications were reported by John et al in their study. These modifications may have prevented the restoration of biocompatibility. Their hypothesis that biocompatibility reduction is caused by surface alteration during the decontamination procedure has to be further investigated by using powders with smaller diameters and

softer materials.

Our findings are consistent with the study by Tastede et al, which demonstrated a higher biocompatibility of discs decontaminated with airflow and erythritol than the untreated discs.<sup>17</sup>

The results of the profilometric analysis showed that amplitude parameters of surface roughness did not significantly change irrespective of the tested specimen, a result that is in accordance with a recent study evaluating Ra values after sterilization by autoclaving.<sup>18</sup> Furthermore, this finding enhances our results as it concerns the restored biocompatibility of discs treated with airflow. Concerning disinfected discs, the only statistically significantly lower value compared to both sterile and autoclaved discs was Ssc. Ssc provides information on the degree of elastic and plastic deformation of a surface under various loading situations, which is helpful in estimating the friction and wear characteristics of a system.<sup>19</sup> The Hybrid parameters of surface roughness have not been investigated yet in discs decontaminated with airflow in research studies, so further evaluation would be beneficial.

Regarding ALP expression, an increase was revealed on days 7 and 14 in all experimental groups. ALP is an early marker of differentiation and a good indicator of bone formation, and its values are expected to increase in cultures on sterile surfaces. However, ALP expression presented no significant differences between sterile and decontaminated implant surfaces for most timepoints. The only statistically significant difference found favored decontaminated surfaces where ALP expression was higher in the cells of group II compared to cells cultured on sterile discs. This interesting finding verifies the restoration of biocompatibility on a molecular level. The possible positive effect of airflow application with erythritol powder on surface characteristics (i.e., wettability, surface free energy, and chemical composition) should be further investigated.

Laser irradiation with a diode (810 nm) offered significant benefits in terms of the differentiation of osteoblast-like cells in both sterile and decontaminated titanium surfaces. All evaluated genes, both early and late markers of differentiation were expressed more intensely when cell cultures were treated with low-level laser irradiation. In several cases, differences between groups treated with or without laser for both sterile and disinfected implant surfaces reached a statistical significance in favor of laser application.

More specifically, laser application led to an overexpression of ALP in cells cultured on sterile and disinfected surfaces 7 and 14 days after the treatment. This difference reached statistical significance for laser-treated cells on sterile discs on day 7. TGF- $\beta$ 1, which is produced by osteoblasts and increases the number of pro-osteoblast cells, is a transforming growth factor that activates the expression of extracellular matrix proteins,



collagen synthesis by osteoblasts, and ALP activity.<sup>20</sup> TGF- $\beta$ 1 was also expressed to a higher extent in laser-treated cultures on sterile and decontaminated surfaces 7 and 14 days after the treatment. This difference was also statistically significant for laser-treated MG63 cells cultured on sterile titanium surfaces. Accordingly, Runx-2, which is necessary for mesenchymal cells to commit to osteoblast lineage cells,<sup>21</sup> was statistically significantly overexpressed in osteoblast-like cells cultured on decontaminated titanium surfaces and treated with LLLT compared to non-irradiated cells cultured on decontaminated surfaces on day 14.

The biomodulative effect of LLLT was further supported by our findings regarding BMP-7 expression. BMP-7 promotes osteoblast differentiation and increases the expression of ALP.<sup>22</sup> After the decontamination of titanium surfaces, irradiated cultured cells expressed BMP-7 at a statistically significantly higher level compared to non-irradiated cells 7 and 14 days after the treatment.

Finally, OSC gene expression, which is observed with the initiation of mineral deposition in osteoid by mature osteoblasts representing a late differentiation marker, was found statistically significantly higher for laser-treated cells cultured in both sterile and disinfected titanium surfaces 14 and 21 days after the treatment.

The biomodulatory effect of various wavelengths on osteoblast-like cells cultured on sterile surfaces has also been supported by other studies. As it concerns rough surfaces,

Khandra et al. examined how the GaAlAs diode laser (830 nm) affected TGF- $\beta$ 1 synthesis, attachment, and differentiation.<sup>10</sup> The findings of this study demonstrated that LLLT considerably improved cellular attachment, while after 96 hours, enhanced cell growth was seen in the groups who had received irradiation. Additionally, Petri et al evaluated how human osteoblastic cells cultivated on titanium responded to the GaAlAs diode laser (780 nm) on days 3 and 7.<sup>11</sup> The findings showed that LLLT-treated cells had greater levels of ALP, OSC, bone sialoprotein (BSP), and BMP-7 expression.

When it comes to smooth surfaces, Karoussis et al proved that Nd: YAG radiation (1064 nm) of MG63 cells resulted in faster proliferation and differentiation compared with non-irradiated surfaces.<sup>12</sup>

In this *in vitro* model, there are a few limitations and practical implications that should be considered, as actual clinical situations cannot be represented. More specifically, the interactions between microbes and the living human tissues, the complexity of host immunity, the variety of risk factors for peri-implant pathology, and conditions that may alter the host response cannot be directly transferred in an *in vitro* model. Furthermore, treatment outcomes are influenced by additional parameters, such as implant surface properties, peri-

implant defect configurations, anatomical limitations of the oral cavity, the presence of suprastructure, or the presence of blood and saliva that may hinder the accessibility to infected implant surfaces.

Despite the aforementioned limitations, this study used discs with the same SLA surface as the implants used in the clinical practice, while the polymicrobial biofilm used mimicked the environment of the oral cavity in case of peri-implantitis. Moreover, cell viability and proliferation were assessed by the MTT assay, which is the most common and reliable method for assessing cell viability, and it was also confirmed by the use of FDA/PI fluorescent dyes. Finally, the study assessed five different genes to obtain all the available information about osteoblast differentiation in every experimental group through time. Nevertheless, clinical relevance remains challenging and further investigation is needed for a better understanding of the events taking place in the true biological site in the human body in case of peri-implantitis.

## Conclusion

Within the limits of the present *in vitro* study, the use of airflow with erythritol powder seemed to be efficient in the decontamination of the infected titanium discs and might be effective in restoring biocompatibility in SLA titanium surfaces. Photomodulation with a laser (810 nm) promoted osteoblastic differentiation in both sterile and disinfected titanium surfaces. Further studies are required to support the beneficial biomodulatory effect of combined airflow decontamination with photomodulation and possibly contribute to the development of a particular and successful treatment protocol for peri-implantitis.

## Acknowledgments

We gratefully acknowledge the profilometric analysis performed by Professor Spiros Zinelis, Professor in the School of Dentistry, National and Kapodistrian University of Athens, Department of Biomaterials.

## Authors' Contribution

**Conceptualization:** Evangelia P. Zampa, Ioannis K. Karoussis.

**Data curation:** Evangelia P. Zampa, Kyriaki Kyriakidou, Ioannis K. Karoussis.

**Formal analysis:** Evangelia P. Zampa, Kyriaki Kyriakidou.

**Funding acquisition:** Ioannis K. Karoussis.

**Investigation:** Evangelia P. Zampa, Kyriaki Kyriakidou, Joseph Papaparaskevas, Eudoxie Pepelassi, Ioannis K. Karoussis.

**Methodology:** Evangelia P. Zampa, Kyriaki Kyriakidou, Joseph Papaparaskevas, Ioannis K. Karoussis.

**Project administration:** Evangelia P. Zampa, Ioannis K. Karoussis.

**Resources:** Ioannis K. Karoussis, Joseph Papaparaskevas.

**Software:** Kyriaki Kyriakidou.

**Supervision:** Ioannis K. Karoussis.

**Validation:** Ioannis K. Karoussis, Evangelia P. Zampa, Eudoxie Pepelassi.

**Visualization:** Evangelia P. Zampa, Eudoxie Pepelassi, Ioannis K. Karoussis.

**Writing—original draft:** Evangelia P. Zampa.

**Writing—review & editing:** Ioannis K. Karoussis, Evangelia P. Zampa.

### Competing Interests

The authors have stated explicitly that there are no conflicts of interest in connection with this article.

### Ethical Approval

Not applicable.

### References

- Schwarz F, Derks J, Monje A, Wang HL. Peri-implantitis. *J Clin Periodontol*. 2018;45 Suppl 20:S246-s66. doi: [10.1111/jcpe.12954](https://doi.org/10.1111/jcpe.12954).
- Diaz P, Gonzalo E, Villagra LJG, Miegimolle B, Suarez MJ. What is the prevalence of peri-implantitis? A systematic review and meta-analysis. *BMC Oral Health*. 2022;22(1):449. doi: [10.1186/s12903-022-02493-8](https://doi.org/10.1186/s12903-022-02493-8).
- Tong Z, Fu R, Zhu W, Shi J, Yu M, Si M. Changes in the surface topography and element proportion of clinically failed SLA implants after in vitro debridement by different methods. *Clin Oral Implants Res*. 2021;32(3):263-73. doi: [10.1111/clr.13697](https://doi.org/10.1111/clr.13697).
- Cosgarea R, Rocuzzo A, Jepsen K, Sculean A, Jepsen S, Salvi GE. Efficacy of mechanical/physical approaches for implant surface decontamination in non-surgical submarginal instrumentation of peri-implantitis. A systematic review. *J Clin Periodontol*. 2023;50 Suppl 26:188-211. doi: [10.1111/jcpe.13762](https://doi.org/10.1111/jcpe.13762).
- Ramanauskaitė A, Schwarz F, Cafferata EA, Sahrman P. Photo/mechanical and physical implant surface decontamination approaches in conjunction with surgical peri-implantitis treatment: a systematic review. *J Clin Periodontol*. 2023;50 Suppl 26:317-35. doi: [10.1111/jcpe.13783](https://doi.org/10.1111/jcpe.13783).
- Baima G, Citterio F, Romandini M, Romano F, Mariani GM, Buduneli N, et al. Surface decontamination protocols for surgical treatment of peri-implantitis: a systematic review with meta-analysis. *Clin Oral Implants Res*. 2022;33(11):1069-86. doi: [10.1111/clr.13992](https://doi.org/10.1111/clr.13992).
- Fischer KR, Büchel J, Gubler A, Liu CC, Sahrman P, Schmidlin PR. Nonsurgical cleaning potential of deep-threaded implants and titanium particle release: a novel in vitro tissue model. *Clin Oral Implants Res*. 2023;34(5):416-25. doi: [10.1111/clr.14045](https://doi.org/10.1111/clr.14045).
- Stein JM, Conrads G, Abdelbary MMH, Yekta-Michael SS, Buttler P, Glock J, et al. Antimicrobial efficiency and cytocompatibility of different decontamination methods on titanium and zirconium surfaces. *Clin Oral Implants Res*. 2023;34(1):20-32. doi: [10.1111/clr.14014](https://doi.org/10.1111/clr.14014).
- Matsubara VH, Leong BW, Leong MJL, Lawrence Z, Becker T, Quaranta A. Cleaning potential of different air abrasive powders and their impact on implant surface roughness. *Clin Implant Dent Relat Res*. 2020;22(1):96-104. doi: [10.1111/cid.12875](https://doi.org/10.1111/cid.12875).
- Khadra M, Lyngstadaas SP, Haanaes HR, Mustafa K. Effect of laser therapy on attachment, proliferation and differentiation of human osteoblast-like cells cultured on titanium implant material. *Biomaterials*. 2005;26(17):3503-9. doi: [10.1016/j.biomaterials.2004.09.033](https://doi.org/10.1016/j.biomaterials.2004.09.033).
- Petri AD, Teixeira LN, Crippa GE, Beloti MM, de Oliveira PT, Rosa AL. Effects of low-level laser therapy on human osteoblastic cells grown on titanium. *Braz Dent J*. 2010;21(6):491-8. doi: [10.1590/s0103-64402010000600003](https://doi.org/10.1590/s0103-64402010000600003).
- Karoussis IK, Kyriakidou K, Psarros C, Lang NP, Vrotsos IA. Nd:YAG laser radiation (1.064 nm) accelerates differentiation of osteoblasts to osteocytes on smooth and rough titanium surfaces in vitro. *Clin Oral Implants Res*. 2017;28(7):785-90. doi: [10.1111/clr.12882](https://doi.org/10.1111/clr.12882).
- Kommerein N, Stumpp SN, Mücken M, Ehlert N, Winkel A, Häussler S, et al. An oral multispecies biofilm model for high content screening applications. *PLoS One*. 2017;12(3):e0173973. doi: [10.1371/journal.pone.0173973](https://doi.org/10.1371/journal.pone.0173973).
- Bourouni I, Kyriakidou K, Fourmousis I, Vrotsos IA, Karoussis IK. Low level laser therapy with an 810-nm diode laser affects the proliferation and differentiation of premature osteoblasts and human gingival fibroblasts in vitro. *J Lasers Med Sci*. 2021;12:e33. doi: [10.34172/jlms.2021.33](https://doi.org/10.34172/jlms.2021.33).
- Lerman MJ, Lembong J, Muramoto S, Gillen G, Fisher JP. The evolution of polystyrene as a cell culture material. *Tissue Eng Part B Rev*. 2018;24(5):359-72. doi: [10.1089/ten.TEB.2018.0056](https://doi.org/10.1089/ten.TEB.2018.0056).
- John G, Becker J, Schwarz F. Effectivity of air-abrasive powder based on glycine and tricalcium phosphate in removal of initial biofilm on titanium and zirconium oxide surfaces in an ex vivo model. *Clin Oral Investig*. 2016;20(4):711-9. doi: [10.1007/s00784-015-1571-8](https://doi.org/10.1007/s00784-015-1571-8).
- Tastepe CS, Lin X, Donnet M, Doulabi BZ, Wismeijer D, Liu Y. Re-establishment of biocompatibility of the in vitro contaminated titanium surface using osteoconductive powders with air-abrasive treatment. *J Oral Implantol*. 2018;44(2):94-101. doi: [10.1563/aaid-joi-D-17-00128](https://doi.org/10.1563/aaid-joi-D-17-00128).
- Sousa V, Mardas N, Spratt D, Hassan IA, Walters NJ, Beltrán V, et al. The effect of microcosm biofilm decontamination on surface topography, chemistry, and biocompatibility dynamics of implant titanium surfaces. *Int J Mol Sci*. 2022;23(17):10033. doi: [10.3390/ijms231710033](https://doi.org/10.3390/ijms231710033).
- Blateyron F, Caulcutt A. 3D imaging and analysis. *Imaging Microsc*. 2006;8(3):42-3. doi: [10.1002/imic.200790094](https://doi.org/10.1002/imic.200790094).
- Xu X, Zheng L, Yuan Q, Zhen G, Crane JL, Zhou X, et al. Transforming growth factor- $\beta$  in stem cells and tissue homeostasis. *Bone Res*. 2018;6:2. doi: [10.1038/s41413-017-0005-4](https://doi.org/10.1038/s41413-017-0005-4).
- Komori T. Regulation of proliferation, differentiation and functions of osteoblasts by Runx2. *Int J Mol Sci*. 2019;20(7):1694. doi: [10.3390/ijms20071694](https://doi.org/10.3390/ijms20071694).
- Shen B, Wei A, Whittaker S, Williams LA, Tao H, Ma DD, et al. The role of BMP-7 in chondrogenic and osteogenic differentiation of human bone marrow multipotent mesenchymal stromal cells in vitro. *J Cell Biochem*. 2010;109(2):406-16. doi: [10.1002/jcb.22412](https://doi.org/10.1002/jcb.22412).